INTERPRETATION OF FIRST-ARRIVAL TRAVEL TIMES WITH WAVEPATH EIKONAL TRAVELTIME INVERSION AND WAVEFRONT REFRACTION METHOD

Siegfried R. Rohdewald, Intelligent Resources Inc., Vancouver B.C., Canada

Abstract

We describe blind interpretation of the synthetic traveltime dataset, made available by Colin Zelt for the SAGEEP 2011 "Seismic Refraction Shootout" session. A 1D initial model (with horizontal layering, parallel to smoothed topography) is obtained automatically from the traveltimes, without requiring the user to assign first breaks to assumed refractors. This initial model is then iteratively refined with WET (Wavepath Eikonal Traveltime inversion: forward model synthetic traveltimes with Eikonal solver, back-project misfit along wavepaths aka Fresnel volumes, in a SIRT-like algorithm).

Alternatively, traveltimes are interpreted with WR (Wavefront Refraction, layer-based ray inversion) method. For WR, first breaks need to be assigned to refractors interactively. WR has problems with imaging faults, pinchouts, outcrops and other velocity anomalies, which violate the WR assumption of laterally continuous layers. And the assignment of first breaks to hypothetical and mathematically idealized refractors is subjective and non-unique. But WR is still useful to detect lateral change of velocity, independent of WET.

Artefacts of the 1D initial model (horizontal layering in basement) are progressively removed, with increasing number of WET iterations. Fit of WET model to WR interpretation (fault in basement) improves with increasing iteration count, even after the RMS error stops decreasing. This demonstrates that using solely the RMS error as a criterion for determining the optimum number of WET iterations is unreliable, and may stop WET prematurely. We propose the following criteria, to determine the optimum number of WET iterations : I. explain traveltimes with smooth minimum-structure model, II. minimum correlation of final model with layering of initial model, III. reasonable fit with WR interpretation, and IV. small RMS error. Also, we match areas of low ray coverage to apparent low-velocity zones in the sedimentary overburden and depressions in the bedrock surface.

Introduction

Wavepath Eikonal Traveltime Inversion

WET inversion (Schuster, 1993) uses the Fresnel volume approach (Watanabe, 1999) to model propagation of first-break energy, in a physically meaningful way. While ray-tracing methods assume that the frequency of the source signal is infinite and model wave propagation along "thin rays", WET partially models finite-frequency effects such as diffraction and scattering, using wavepaths aka Fresnel volumes or "fat rays" (Husen, 2001). For each source and receiver, WET forward models traveltimes to all grid nodes with an Eikonal solver (Lecomte, 2000) and back-projects traveltime residuals along wavepaths, in a SIRT-like algorithm. WET naturally smoothes the tomogram, but requires careful first break picking. Bad picks can result in artefacts ("engraving" of wavepaths in tomogram), especially in low-coverage situations (low ratio of shots to receivers). As shown with interpretation of synthetic data (Sheehan, 2005; Jansen, 2010), refraction tomography and WET (with a 1D initial model) work well in many situations where conventional layer-based refraction methods fail. Refraction tomography blurs sharp velocity contrasts, and images them with gradients.

Wavefront Refraction Method

Wavefront Refraction (WR) is a layer-based ray inversion method, and has been described by (Jones, 1985), (Brueckl, 1987) and (Ali Ak, 1990). WR requires the user to interactively assign first breaks to assumed refractors. Conventional methods such as WR, Plus-Minus (Hagedoorn, 1959) and GRM (Generalized Reciprocal Method) (Palmer, 1981) are based on the often unrealistic assumption that the subsurface can be modeled with a few laterally continuous layers with no vertical velocity gradient. Such layers are mathematically idealized refractors, with constant layer-internal velocity below constant inline offset. Faults, velocity inversions, local velocity anomalies, pinchouts, outcrops and vertical velocity gradients within layers often make the interactive assignment of first breaks to hypothetical refractors difficult and ambiguous.

(Ali Ak, 1990) used Palmer's synthetic models to compare WR with Plus-Minus and GRM. WR can image irregular refractor surfaces and detects sudden lateral change in velocity. WR depth calculations are independent of the refractor velocity.

Processing and results

We processed the traveltime data with the Smooth inversion method (Rohdewald, 2010), as offered with Rayfract® software version 3.18. Smooth inversion first automatically determines a 1D initial model directly from the picked traveltimes, with the DeltatV method (Gebrande, 1985 and 1986; Gibson, 1979). This 1D initial model then is iteratively refined with 2D WET tomographic inversion.

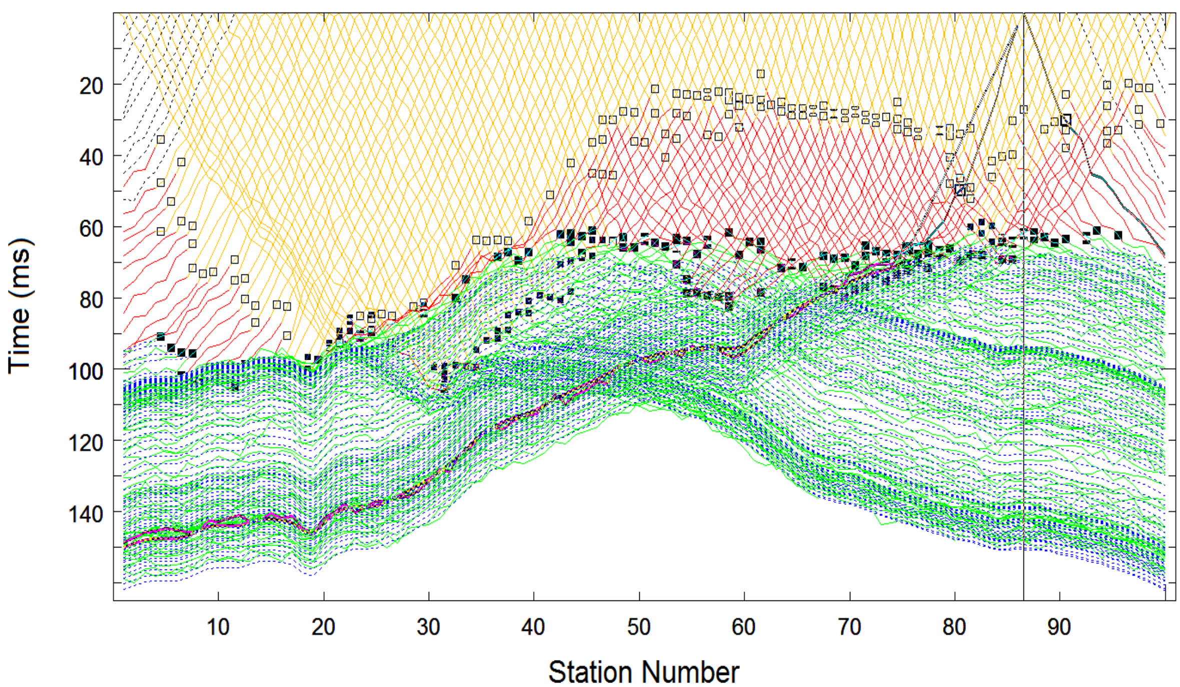

Figure 1: Shot-sorted traveltime curves, with interactive mapping of traces to refractors. Outlined squares separate direct wave (yellow) from overburden refractor (red). Black squares separate overburden refractor (red) from basement refractor (green). This mapping is not required for Smooth inversion. Dashed blue curves on basement refractor show regressed WR times. Note basement refractor anomalies at station nos. 20 and 60 (depressions on reverse shot curves), and at station no. 30 (forward shot curves). Black squares on reverse shots outline the bottom of the anomaly at station no. 60.

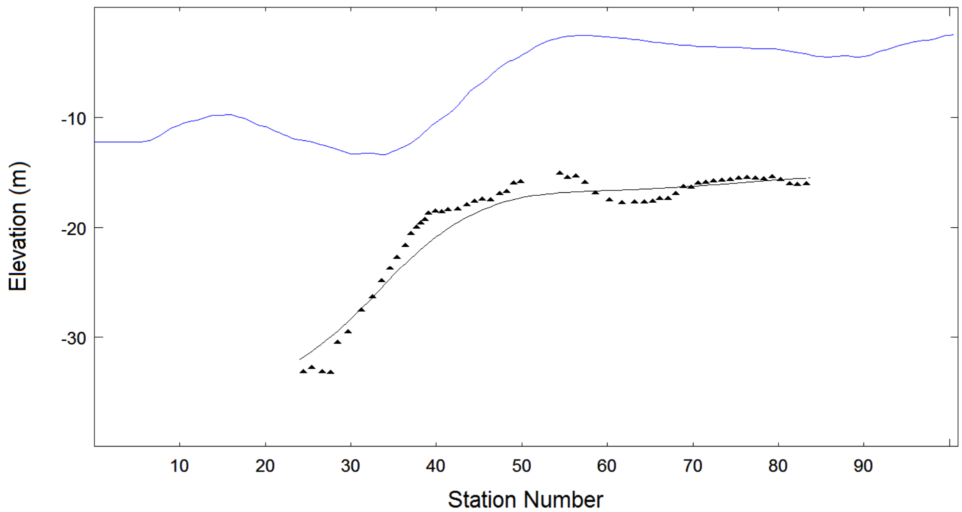

Figure 2: WR depth section, based on assignment of first breaks to refractors as shown in Fig. 1. Blue solid line is first refractor. Black triangles outline estimated shape of basement refractor. Station spacing is 3m. Note basement anomalies (depressions) around station nos. 25 and 63.

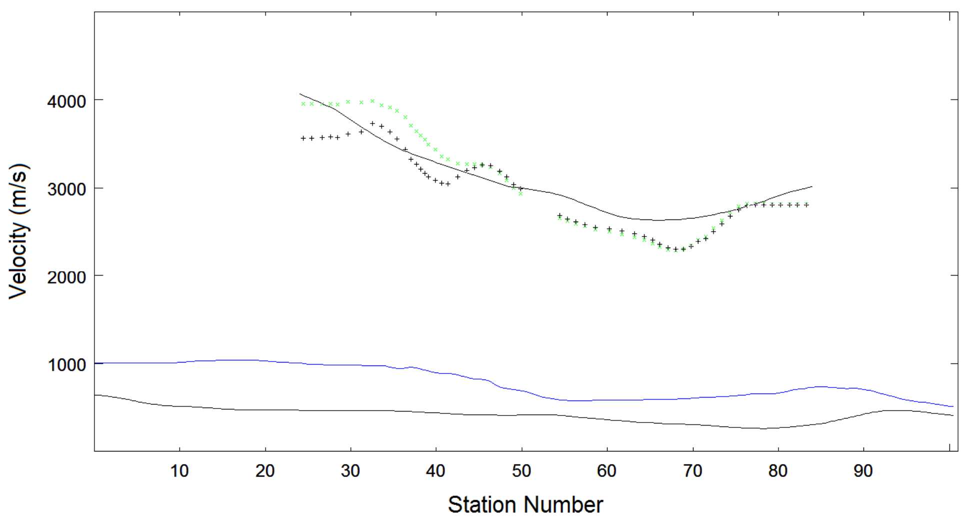

Figure 3: WR velocity section, obtained with depth section shown in Fig. 2. Bottom-most solid curve is direct wave velocity (300 m/s to 600 m/s). Blue solid curve is overburden refractor velocity (500 m/s to 1,000 m/s). Basement refractor velocity (2,300 m/s to 4,000 m/s) is estimated with three different methods (Brueckl, 1987) and shown with black solid curve, black plus-symbols and green crosses. The systematic increase of basement velocity to left of station no. 50 hints at a faulted basement.

Processing Sequence

1. Import ASCII.ASC file with traveltimes and recording geometry into new profile database, with *Header|Profile|Station spacing* set to 3m. Set z coordinate to 0 in *Header|Station* for one station and hit ENTER, to extrapolate coordinates for all stations.
2. Review shot-sorted traveltime curves, shown in Figure 1. Assignment of first breaks to refractors was done in step 6 only, and is not used for Smooth inversion (steps 3 to 5).

3. Run Smooth inversion, with default parameters. Figure 4(a) shows the 1D initial model obtained with Smooth inversion and DeltatV method.
4. Increase WET iteration count to 200 and redo WET inversion, with same 1D initial model as shown in Figure 4(a). For WET output after 200 iterations see Figure 5(a).
5. Redo WET inversion with 1D initial model shown in Figure 4(a), and 999 iterations. For WET output after 999 iterations see Figure 6(a). This step took about 10 hours, on Intel Core i3 CPU.
6. Interactively assign traces to refractors. See Figure 1. This was the most labor-intensive step.
7. WR interpretation. Figure 2 shows WR depth section. Figure 3 shows WR velocity section.
8. Change Smooth inversion parameters, to obtain a different 1D initial model (Figure 4(b)). We limited the maximum exported DeltatV velocity to 3,000 m/s. Also, we smoothed CMP (Common Mid-Point) sorted traveltime curves over adjacent offsets, before DeltatV inversion.
9. Redo WET inversion with initial model shown in Figure 4(b), and 200 WET iterations. See Figure 5(b) for WET output after 200 iterations.
10. Redo WET inversion with initial model shown in Figure 4(b), and 999 WET iterations. See Figure 6(b) for WET output after 999 iterations. This step took about 9 hours, on Intel Core i3.

Interpretation of Results

Artefacts of the 1D initial model (horizontal layering in basement, Figure 4) are progressively removed, with increasing number of WET iterations. Fit of WET model to WR interpretation (fault in basement, Figure 6) improves with increasing iteration count, even after the RMS error stops decreasing.

Setting the initial basement velocity to a constant value smaller than the maximum velocity in the default initial model (Figure 4) can speed up the convergence towards a realistic basement velocity distribution (fault in basement, Figures 5 and 6). Also, initial model artefacts (horizontal layering in basement, Figure 4) can be explicitly removed directly from the initial model, with such a velocity threshold. Our term “basement” means “bedrock”, and “overburden” means “sediments”.

Wavepath coverage does not significantly differ after 200 and 999 iterations (Figure 7). But WET basement velocity structure (fault in basement) obtained after 999 WET iterations (Figure 6) does differ from WET velocity after 200 iterations (Figure 5). Apparently velocity changes in predominantly low-coverage areas, at bottom and edges of tomogram. These changes are visible in the velocity tomogram, but have no meaningful effect on overall summed-up wavepath coverage and RMS error.

The survey objective (Zelt, 2010) is to identify low-velocity zones within the sedimentary layers, as well as features of the bedrock surface and within the bedrock. As shown by (Hickey, 2009a and 2009b; Riddle, 2010), subsurface regions with low WET wavepath coverage can reveal low-velocity anomalies. Figure 7 shows wavepath coverage for our data set. Low coverage areas are visible at bottom of overburden, at offsets 60m and 190m (elevation -20m). The vertical position of the anomaly at offset 60m is not well constrained, since wavepaths and rays in this area are oriented predominantly parallel to each other, in a sub-vertical direction. This causes vertical smearing of resolution (White, 1989). There may be karst-type features (pinnacles) in this overburden region (offset 30m to 120m, at elevation range 0m to -40m). These anomalies are partially visible in Figures 1, 2 and 6 as well. See figure captions.

(Zelt, 2010) mentions that the water table depth varies considerably in the area, between 20m and 100m. This agrees with the strong basement fault shown in our final interpretation (Figure 6).

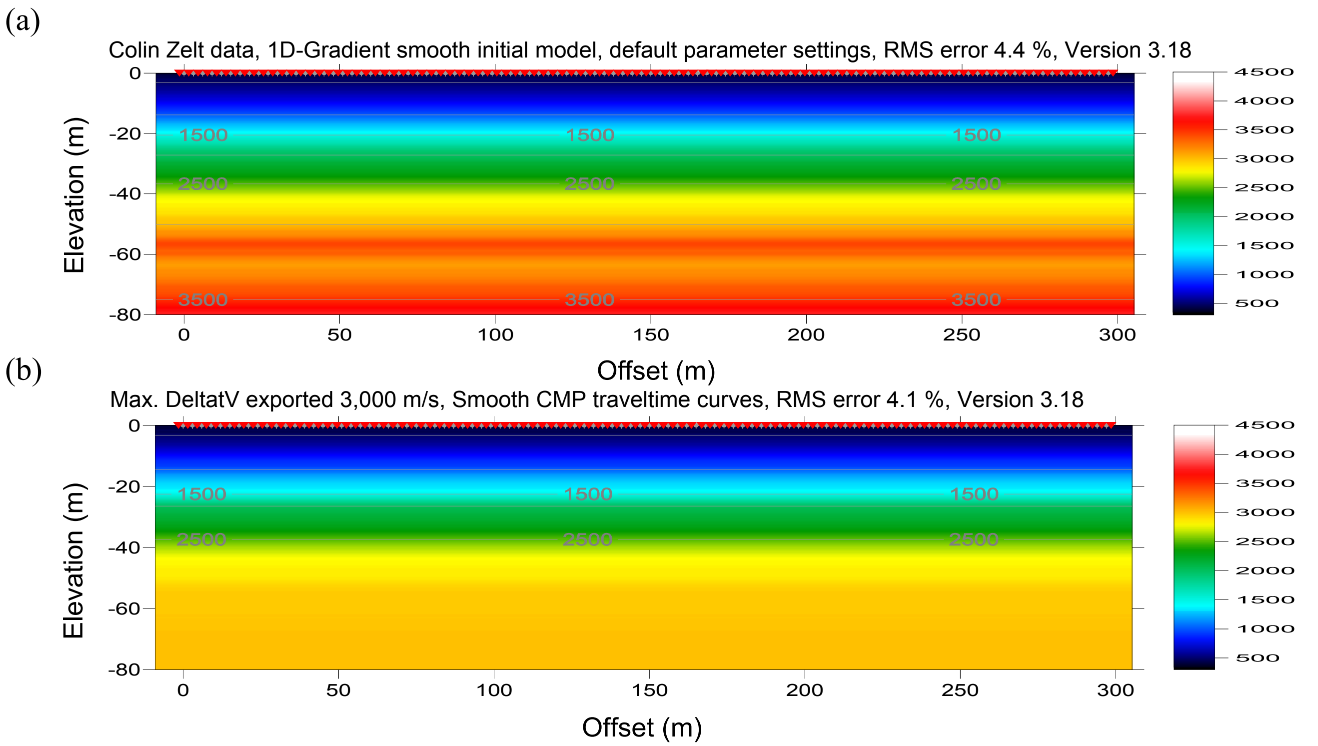

Figure 4: 1D initial velocity (m/s) **(a)** Default parameters. **(b)** Max. exported DeltatV velocity limited to 3,000 m/s, smoothed CMP traveltime curves. Note removed layering artefacts in basement.

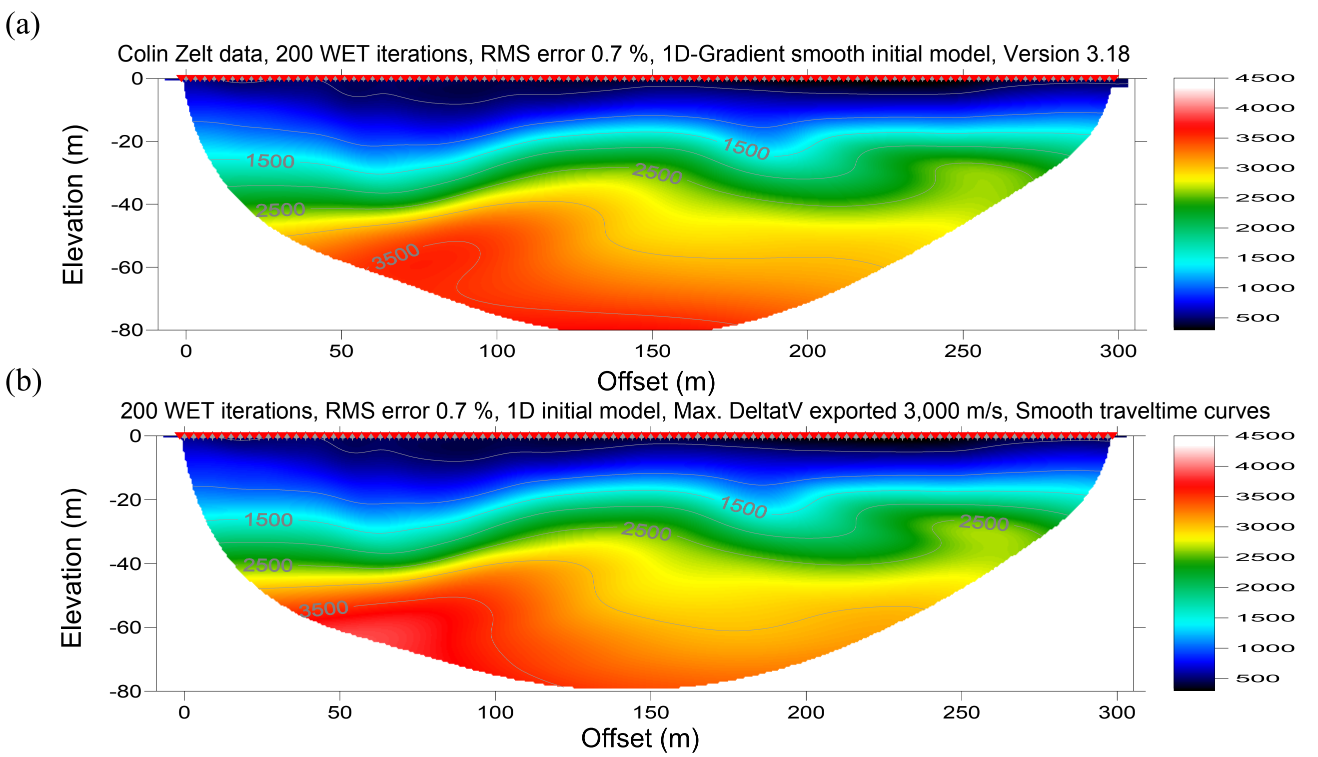

Figure 5: Velocity (m/s) after 200 WET iterations, with initial models from Fig. 4. **(a)** Fig. 4(a) after 200 WET iterations. **(b)** Fig. 4(b) after 200 WET iterations. Basement fault is simpler and better visible, less basement layering artefacts.

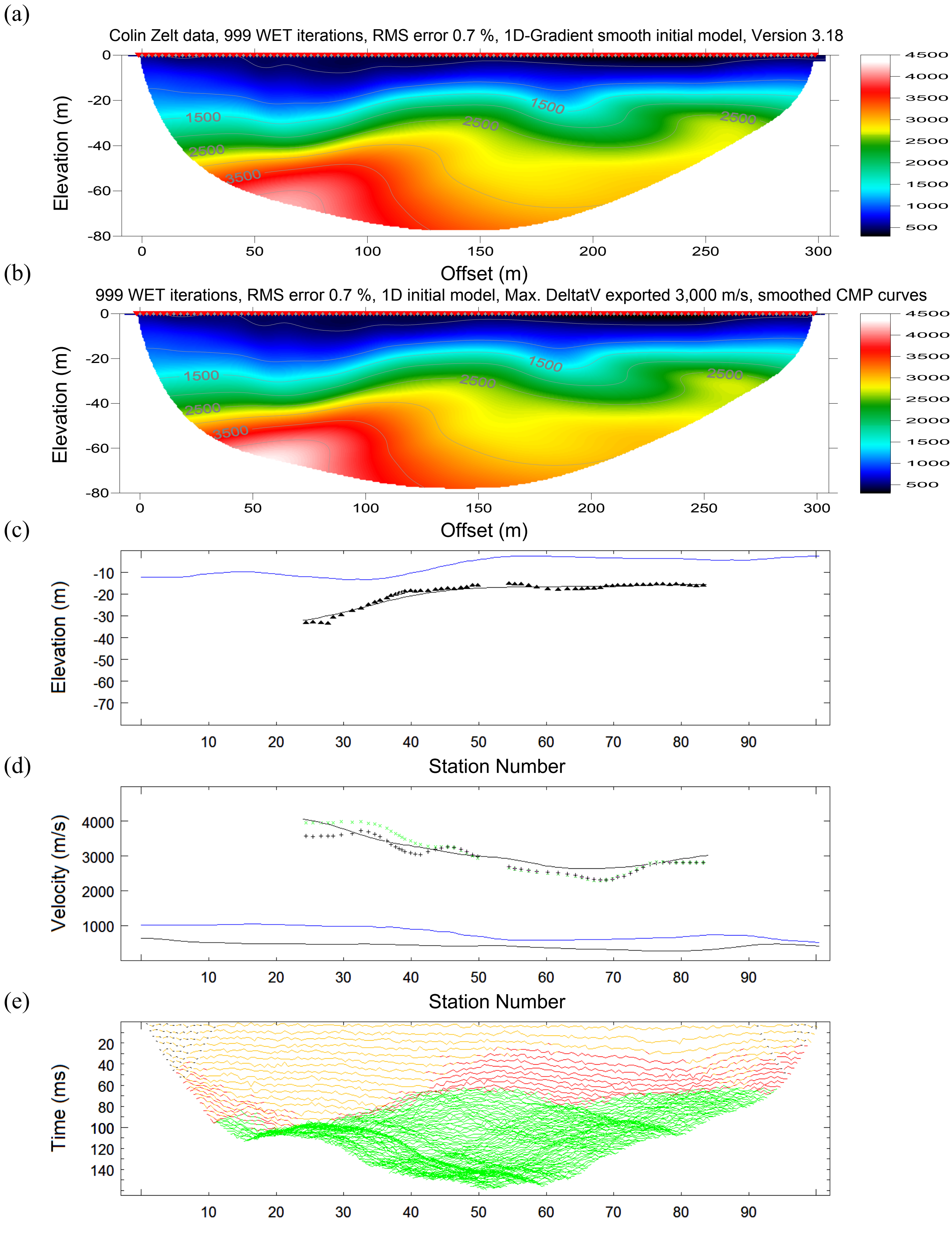
(a)
Colin Zelt data, 999 WET iterations, RMS error 0.7 %, 1D-Gradient smooth initial model, Version 3.18
Elevation (m)
Offset (m)
1500
2500
3500
(b)
999 WET iterations, RMS error 0.7 %, 1D initial model, Max. DeltatV exported 3,000 m/s, smoothed CMP curves
Elevation (m)
Offset (m)
1500
2500
3500
(c)
Elevation (m)
Station Number
(d)
Velocity (m/s)
Station Number
(e)
Time (ms)

Figure 6 (previous page): Velocity tomograms (m/s) after 999 WET iterations, with initial models from Fig. 4. **(a)** Fig. 4(a) after 999 WET iterations. Note slight depressions in 1,500 m/s velocity contour, at offsets 60m and 190m. **(b)** Fig. 4(b) after 999 WET iterations. **(c)** Scaled WR depth section, from Fig. 2. **(d)** Scaled WR velocity section, from Fig. 3. **(e)** Traveltime curves, sorted by common offset. X axis is CMP station number, y axis is time (ms). Assignment of traces to refractors and layer colors as in Fig. 1.

(a)

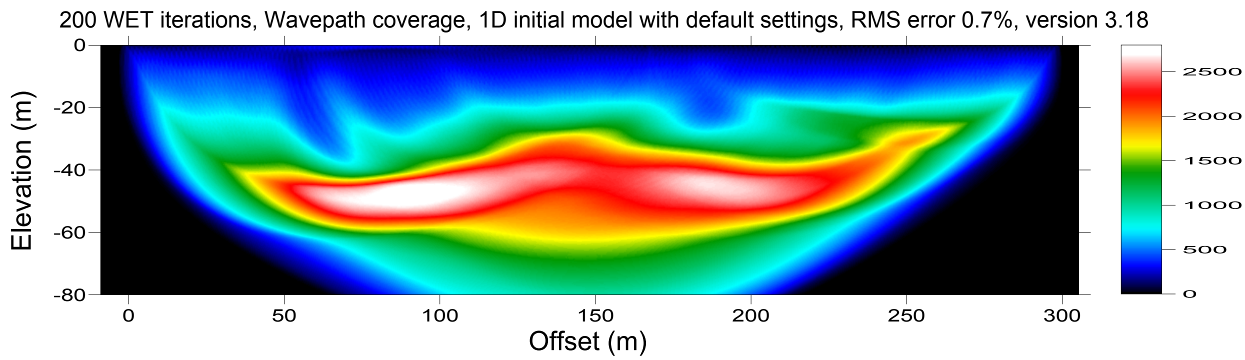

(b)

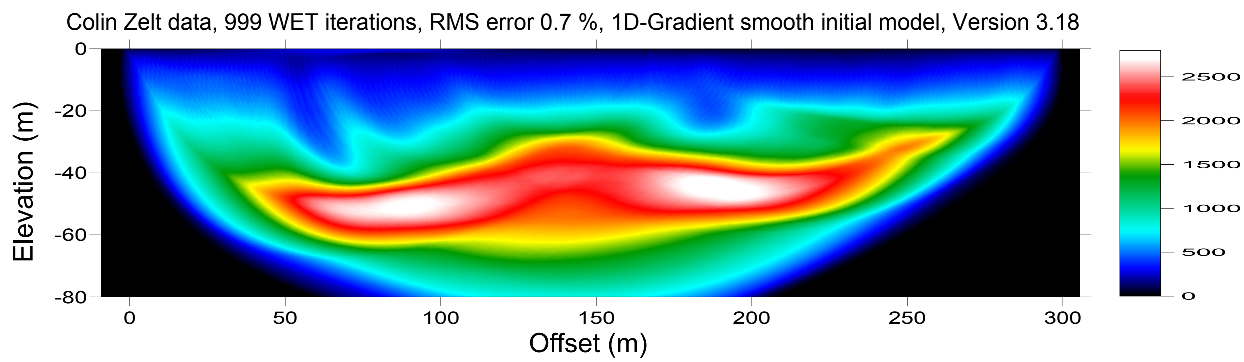

Figure 7: WET wavepath coverage (wavepaths per pixel), with initial model Fig. 4(a). **(a)** Coverage after 200 WET iterations. **(b)** Coverage after 999 WET iterations. Note low-coverage areas at offsets 60m and 190m, and at elevation range -10m to -40m. At offset 90m, there is another depression in surface of basement, at elevation -30m.

Conclusions

We have demonstrated that using solely the RMS error as a criterion for determining the optimum number of iterations for WET (Wavepath Eikonal Traveltime inversion) is unreliable, and may stop WET prematurely. We propose the following criteria, to determine the optimum number of WET iterations : I. explain traveltimes with smooth minimum-structure model, II. minimum correlation with layering of initial model, III. reasonable fit with WR (layer-based Wavefront Refraction) interpretation, and IV. small RMS error of the traveltime residuals.

Also, we have identified two areas of low ray coverage, and visually matched these anomalies to low-velocity regions in the overburden and depressions in the bedrock surface. As shown before in past literature, wavepath and ray coverage may be useful to locate zones of low velocity.

Finally, we have shown that applying a low-pass filter to the initial basement velocity can speed up WET convergence towards a realistic basement velocity distribution.

Acknowledgements

This expanded abstract was first published in Proceedings of SAGEEP, on the 2011 meeting Proceedings CD. We thank EEGS for permission to republish this work.

References

Ali Ak, M., 1990, An analytical raypath approach to the refraction wavefront method, Geophysical Prospecting, Volume 38, 971-982.

Brueckl, E., 1987. The interpretation of traveltime fields in refraction seismology, Geophysical Prospecting, Volume 35, 973-992.

Cerveny, V., Soares, J., 1992. Fresnel volume ray tracing, Geophysics, Volume 57, 902-915.

Gebrande, H., Miller, H., 1985, Refraktionsseismik, in: Angewandte Geowissenschaften II. Ferdinand Enke Verlag, Stuttgart, 226-260. ISBN 3-432-91021-5.

Gebrande, H., 1986, CMP-Refraktionsseismik, in: Seismik auf neuen Wegen. Lothar Dresen, Juergen Fertig, Horst Rueter, Wolfgang Budach, 191-205.

Gibson, B.S., Odegard, M.E., Sutton, G.H., 1979, Nonlinear least-squares inversion of traveltime data for a linear velocity-depth relationship, Geophysics, Volume 44, 185-194.

Hagedoorn, J.G., 1959, The Plus-Minus method of interpreting seismic refraction sections, Geophysical Prospecting, Volume 7, 158-182.

Hickey, C.J., Ekimov, A., Hanson, G.J., Sabatier, J.M., 2009, Time-lapse seismic measurements on a small earthen embankment during an internal erosion experiment, Proceedings of SAGEEP, Fort Worth, TX, May 30-April 3, 144-156, 2009a.

Hickey, C.J., Schmitt, D.R., Sabatier, J.M., Riddle, G., 2009, Seismic measurement for detecting underground high-contrast voids, Proceedings of Symposium on Applications of Geophysics to Environmental and Engineering Problems, Fort Worth, TX, May 30-April 3, 929-936, 2009b.

Husen, S., Kissling, E., 2001, Local earthquake tomography between rays and waves: fat ray tomography, Physics of the earth and Planetary Interiors, Volume 123, 129-149.

Jansen, S., 2010, Parameter investigation for subsurface tomography with refraction seismic data, Master thesis, Niels Bohr Institute, University of Copenhagen.

Jones, G.M., Jovanovich, D. B., 1985, A ray inversion method for refraction analysis, Geophysics, Volume 50, 1701-1720.

Lecomte, I., Gjoystdal, H., Dahle, A., Pedersen, O.C., 2000, Improving modeling and inversion in refraction seismics with a first-order Eikonal solver, Geophysical Prospecting, Vol. 48, 437-454.

Palmer, D., 1981, An Introduction to the generalized reciprocal method of seismic refraction interpretation, Geophysics, Volume 46, 1508-1518.

Riddle, G.I., Hickey, C.J., Schmitt, D.R., 2010, Subsurface tunnel detection using electrical resistivity tomography and seismic refraction tomography: a case study, Proceedings of SAGEEP, Keystone, Colorado, 552-562.

Rohdewald, S., Burton, B., Sheehan, J., Doll, W., 2010, Processing of seismic refraction tomography data, SAGEEP short course notes, Keystone, Colorado.

Schuster, G.T., Quintus-Bosz, A., 1993, Wavepath eikonal traveltime inversion : Theory. Geophysics, Volume 58, 1314-1323.

Sheehan, J.R., Doll, W.E., Mandell, W., 2005, An evaluation of methods and available software for seismic refraction tomography analysis, JEEG, Volume 10(1), 21-34.

Watanabe, T., Matsuoka, T., Ashida, Y., 1999, Seismic traveltime tomography using Fresnel volume approach, SEG Houston 1999 Meeting, Expanded Abstracts.
White, D.J., 1989, Two-dimensional seismic refraction tomography, Geophysical Journal, Volume 97, 223-245.
Zelt, 2010, SAGEEP 2011 Seismic refraction shootout: blind test of methods for obtaining velocity models from first-arrival travel times, http://terra.rice.edu/department/faculty/zelt/sageep2011 .